Science Advances

AAAS

advances.sciencemag.org/cgi/content/full/4/3/eaar3724/DC1

Supplementary Materials for

Anisotropic, lightweight, strong, and super thermally insulating nanowood with naturally aligned nanocellulose

Tian Li, Jianwei Song, Xinpeng Zhao, Zhi Yang, Glenn Pastel, Shaomao Xu, Chao Jia, Jiaqi Dai, Chaoji Chen, Amy Gong, Feng Jiang, Yonggang Yao, Tianzhu Fan, Bao Yang, Lars Wågberg, Ronggui Yang, Liangbing Hu

Published 9 March 2018, *Sci. Adv.* **4**, eaar3724 (2018)
DOI: 10.1126/sciadv.aar3724

This PDF file includes:

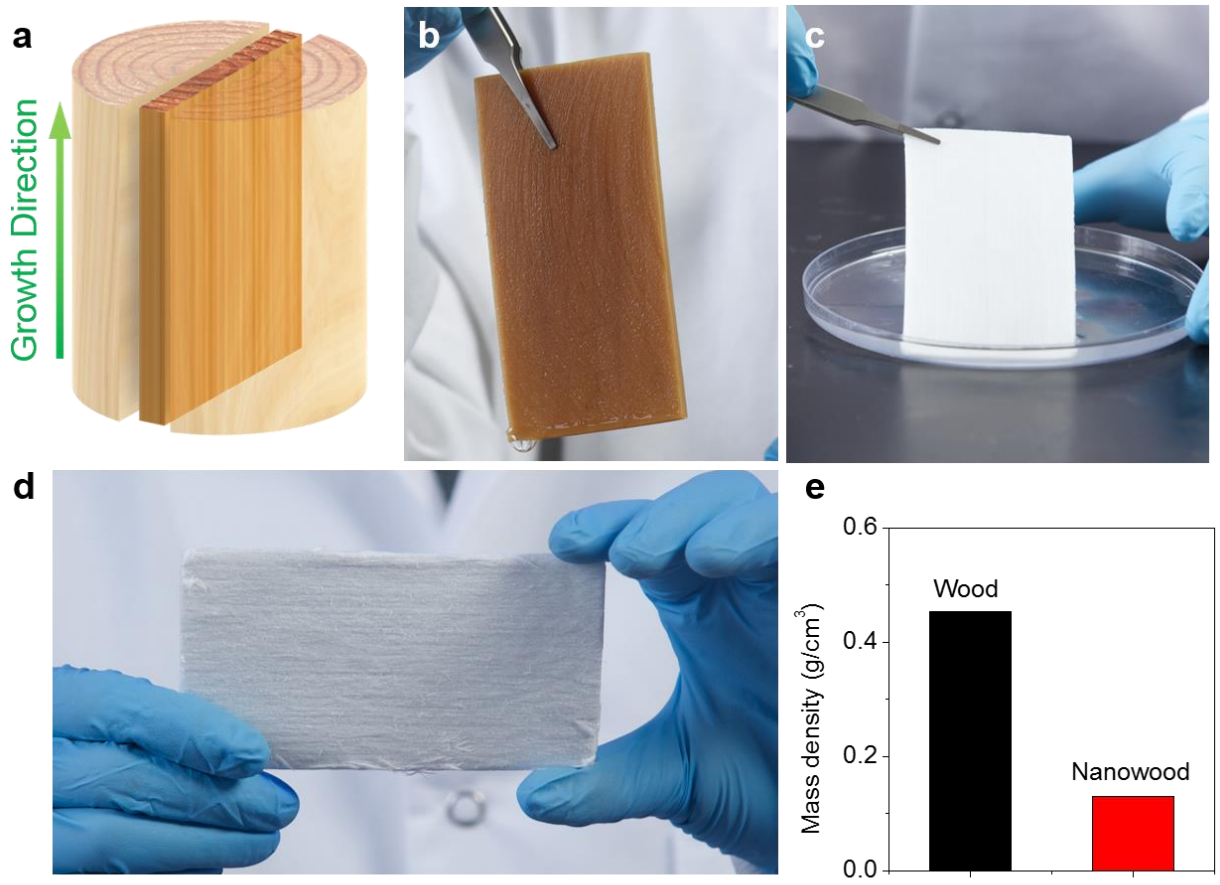

fig. S1. Nanowood is composed of hierarchical aligned nanofibrillar cellulose arrays derived from natural wood. (**a**)(**b**)(**c**) The natural American basswood block is cut vertically along the wood growth direction. Wood microchannels (i.e. the fibrils with their hollow lumen) are naturally aligned, as well as the cellulose nanofibrils inside of the cell walls. The unique structure of American basswood is highly hierarchical in an aligned manner. (**d**) The natural wood can be processed to Nanowood with a well-preserved structure and (**e**) a much lower mass density (70% lower). Our developed process can efficiently remove the lignin and hemicellulose inside the fibril wall and between the fibrils, leaving cellulose as the main component in nanowood. The resulting nanowood can be of a size comparable to that of naturally cut wood block.

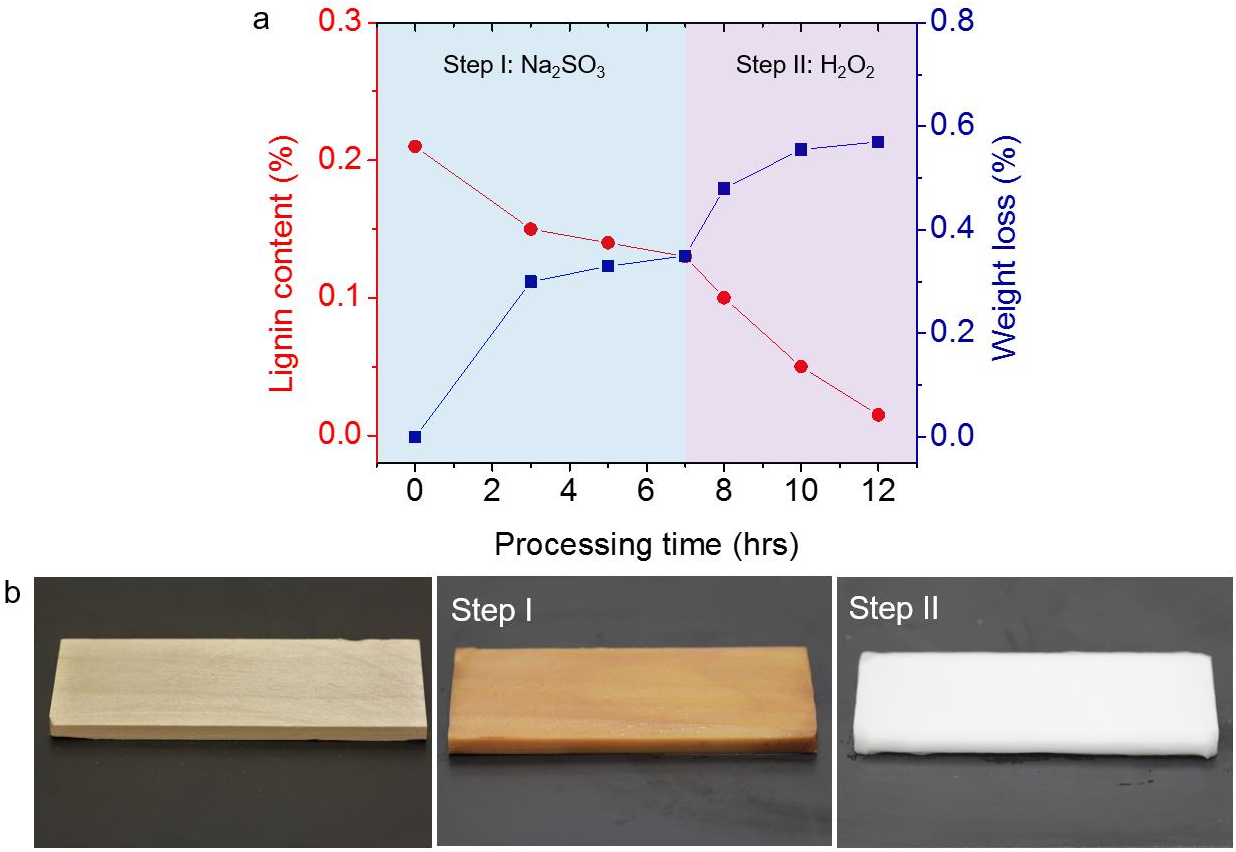

fig. S2. The lignin content and appearance between chemical processes. (**a**) The lignin content change (weight fraction) and overall weight loss of the initial wood specimen during chemical processing. (**b**) Photographic evidence showing the pure white color of the nanowood due to the high reflectivity of visible light, after the two-step chemical process.

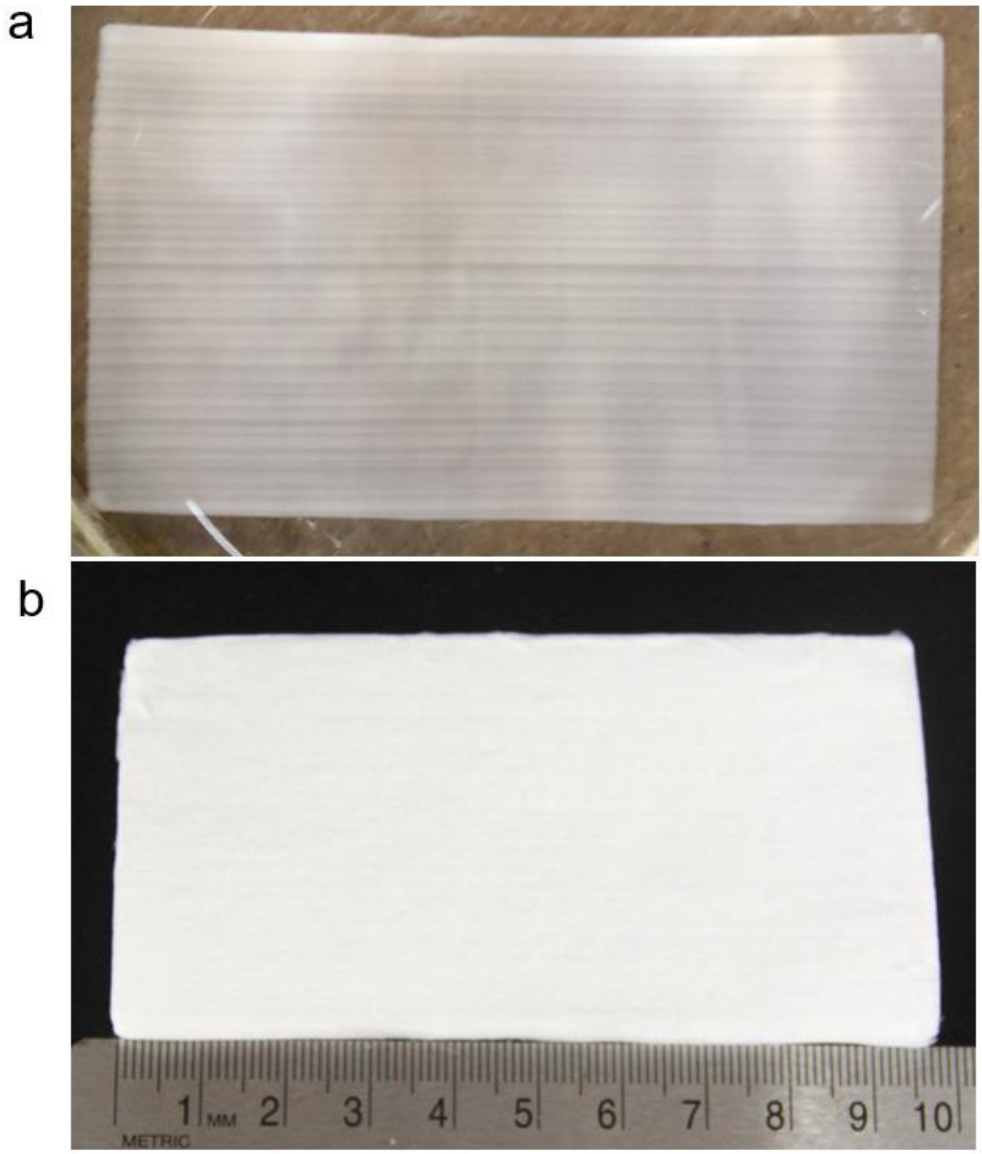

fig. S3. Nanowood drying process.

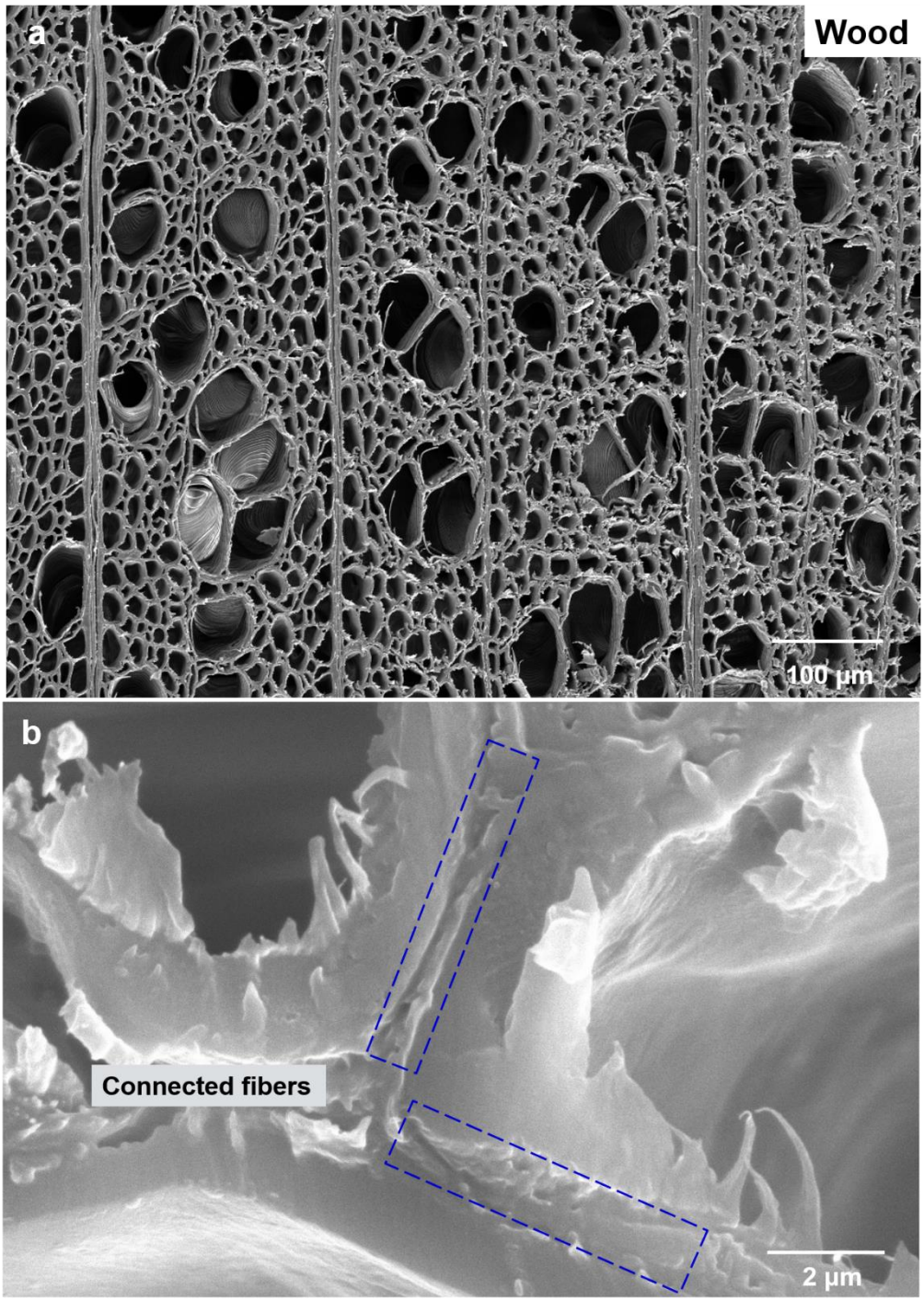

fig. S4. SEM images of natural wood. The wood exhibits aligned fibrils inside the wood structure. The SEM shows a top view of the open and aligned fibrils with hollow lumens. Inset: The lumens adjacent to each other are connected through an intricate pore system**.**

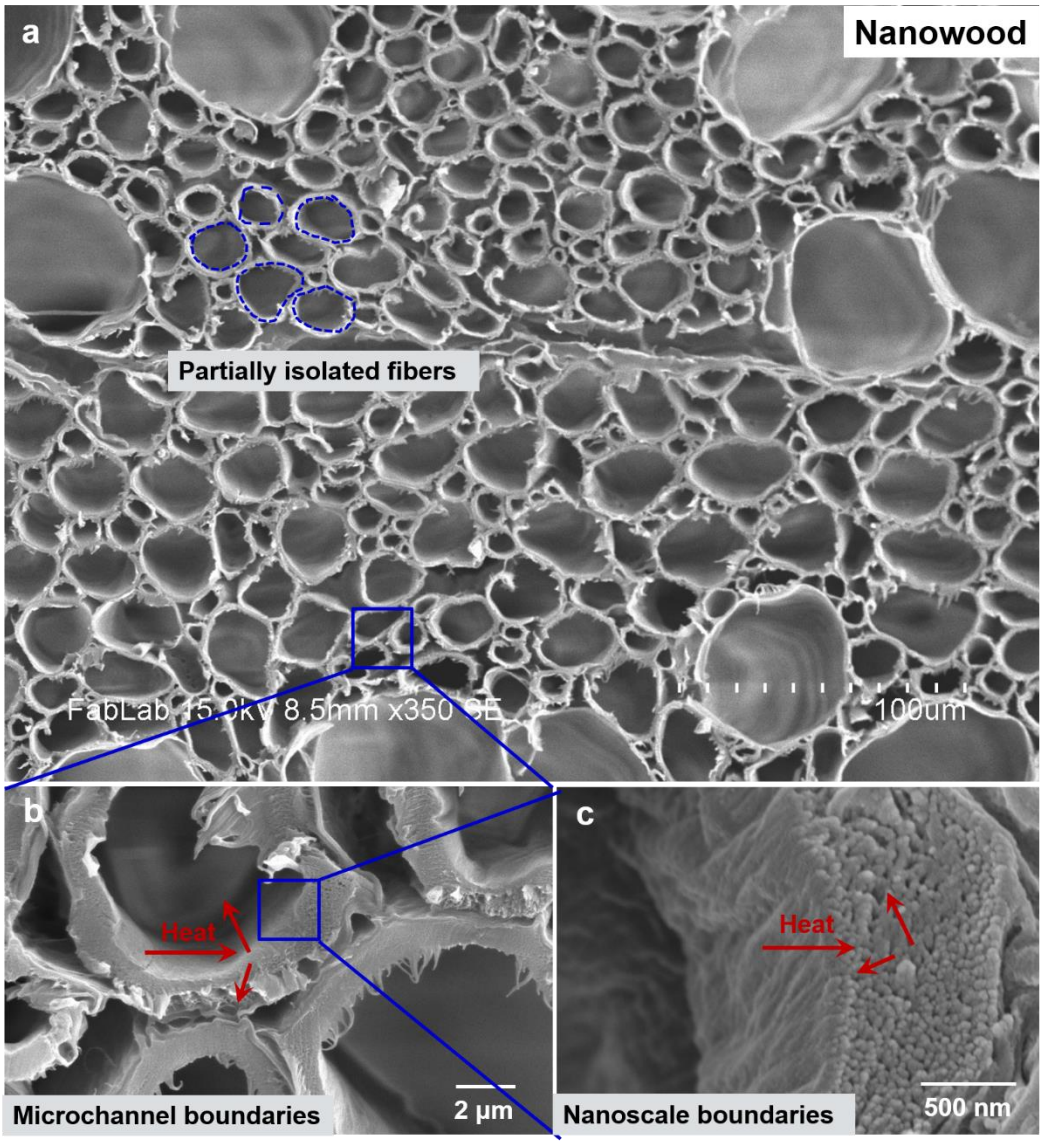

fig. S5. SEM images of nanowood. The alignment of the fibrils is maintained after delignification. However, owing to the purification of the cellulose content, the fibrils become separated and partially detached from each other. The nanofibrils in the fibril walls are more distinct as the intermixed lignin and hemicellulose in between cellulose are removed. The sample was cut before delignification.

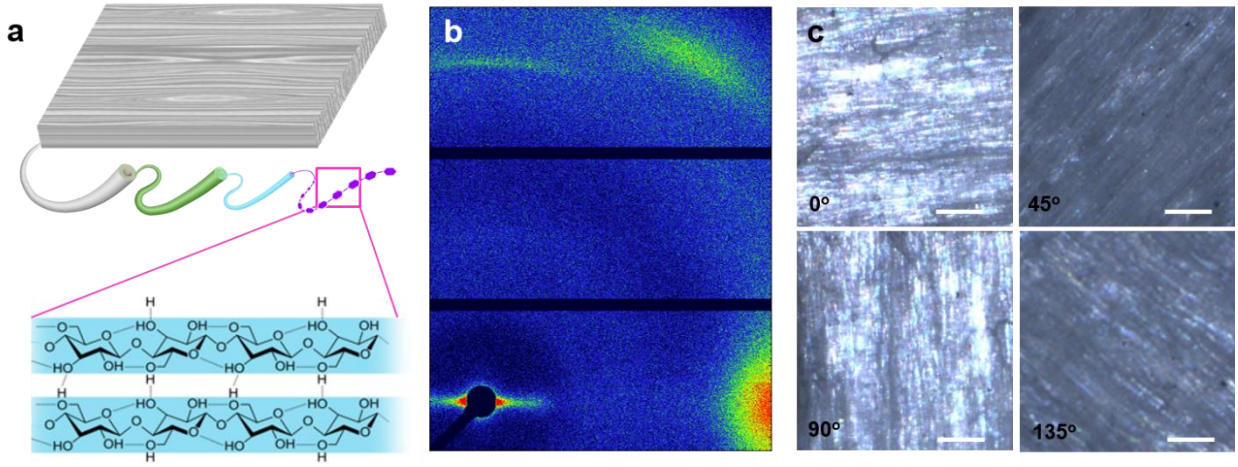

fig. S6. Molecular level alignment in the hierarchal alignment of nanowood. The molecular level alignment stems from the intrinsic parallel orientation of crystalline cellulose molecules. These aligned long-chain cellulose molecules form cellulose fibrils with a diameter of 2 to 4 nm, which are further aligned to form the fibril walls. (**a**) Schematics of the hierarchical structure of nanowood. The molecular chains are aligned within the nanocellulose fibrils. (**b**) SAXS results of nanowood. (**c**) Optical polarization effect of the nanowood surface. Owing to the alignment of the nanofibers, the film appears brightest when the fibers are parallel or perpendicular to the light polarization direction and darker at 45°.

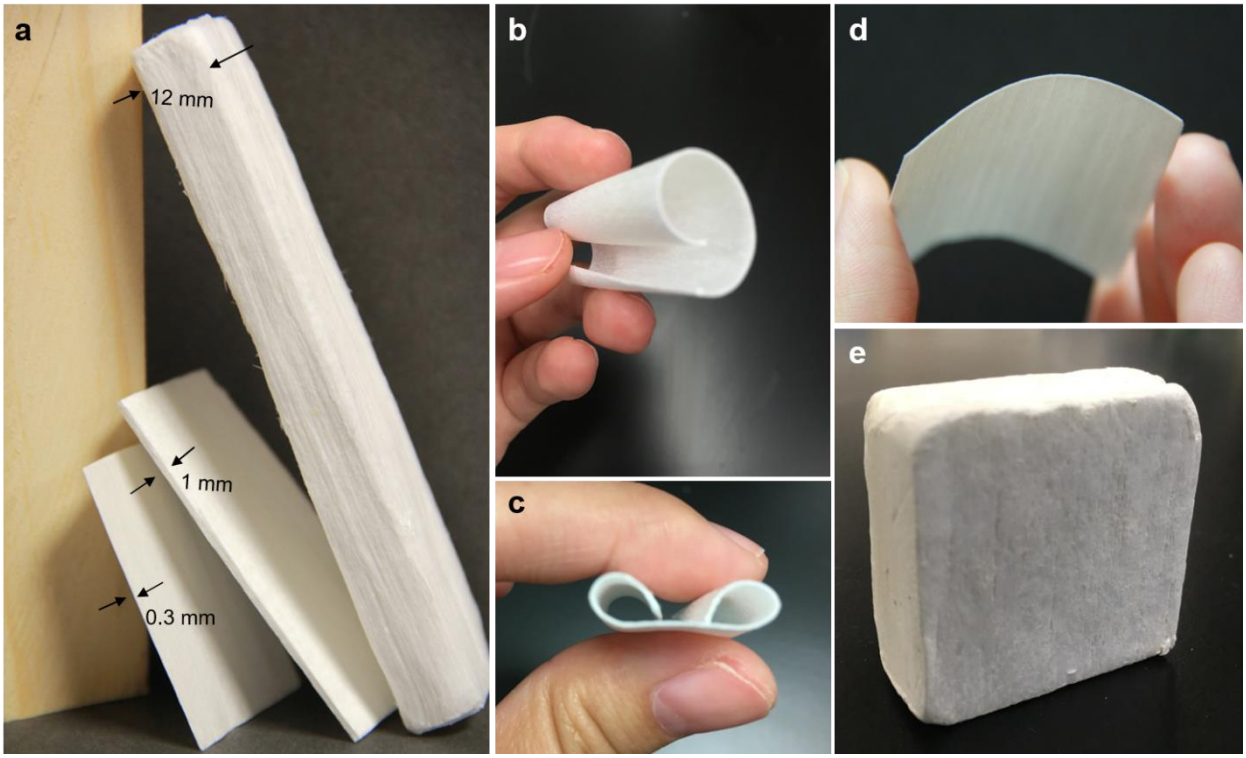

fig. S7. Nanowood samples can be fabricated within a wide size distribution. The flexible and lightweight nanowood can be used as a coating or bulk layer for thermal insulation applications without a significant increase in the respective carbon footprint. As shown, thin slices of nanowood are flexible and can be rolled up without breaking. The nanowood is compact, reliable and manufacturable for large dimensions. It can also be interfaced with existing systems such as building thermal insulation with minimal modifications.

discussion S1. Mechanical property analysis of nanowood

The elementary cellulose fibrils, consisting of hydrogen bonded molecular chains, are highly aligned along the wood growth direction with a small microfibril angle. Given that cellulose is the dominant constituent in the delignified wood, the corresponding toughening and strengthening mechanisms can be understood as follows: removal of lignin and hemicellulose by chemical treatment can increase the interfacial area among nanofibers. At the cellulose nanofiber scale, due to the rich hydroxyl groups in the cellulose molecular chains, the relative sliding among densely packed wood cell walls involves an enormous number of repeating events of hydrogen bond formation, breaking, and reformation. A large interaction area is key to improve the mechanical strength of cellulose-based materials (*64*). Consequently, the nanowood exhibits a high mechanical strength compared to traditional cellulose aerogels or paper (composed of randomly oriented cellulose fibers with much less hydrogen bonding between, typically exhibiting a tensile strength of 250 KPa to 300 KPa) (*65*).

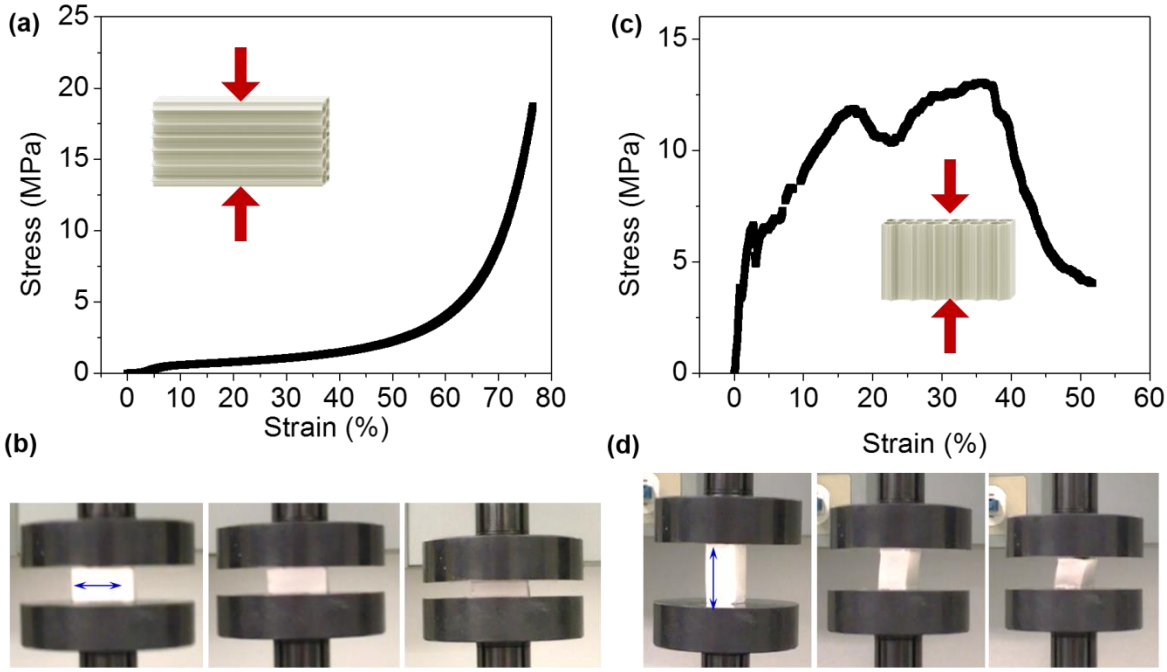

fig. S8. Compressive stress test of nanowood along the axial and radial direction. (**a**) The exponentially increasing stress while pressing along the radial direction. (**b**) Photographs of the radial test process. (**c**) The stress vs strain while pressing along the axial direction. (**d**) Photographs of the axial test process.

The original wood exhibits better mechanical strength compared than nanowood. Lignin functions as “adhesives” in between cellulose nanofibers and is responsible for the good mechanical strength of the original wood. In nanowood, the extraction of lignin and hemicellulose increases the interaction area of the aligned cellulose fibers. The molecular bonding or Van de Waals’ interactions help restore the mechanical strength of nanowood.

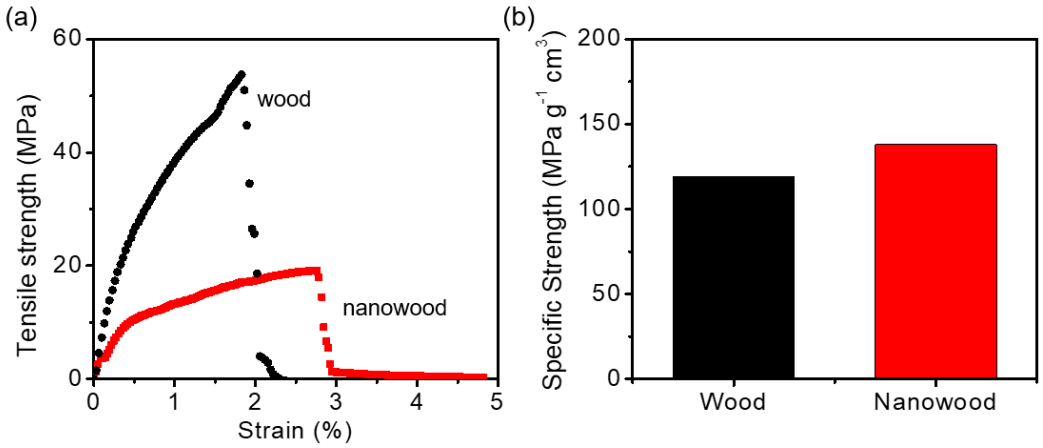

fig. S9. Tensile strength of the nanowood and original wood. (**a**) Tensile strength comparison between nanowood and the original wood. (**b**) Specific strength comparison between nanowood and original wood.

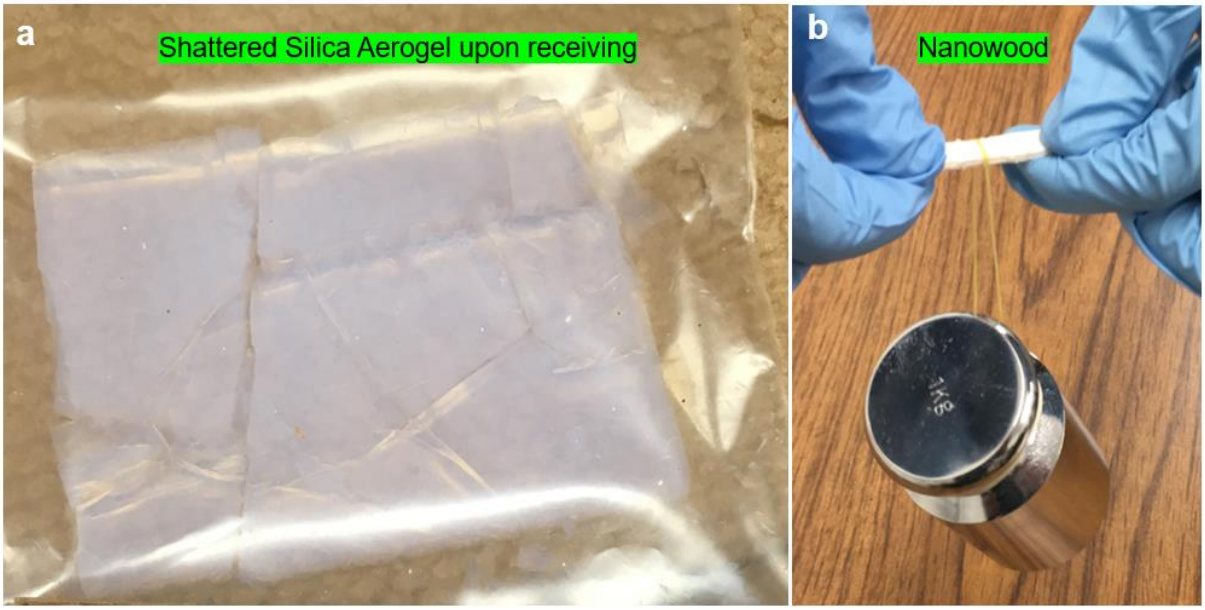

fig. S10. Comparison between commercially available silica aerogel and nanowood. (**a**) To study the existing thermal insulation materials, we bought a silica aerogel tile (retail price $200). Due to the extremely low mechanical strength (fragile), the aerogel arrived shattered due to shipping and handling. This serves as a good example for why silica aerogel is not always a suitable, scalable thermal insulation material due to its brittleness and high cost. (**b**) On the contrary, we show that the nanowood can be much more durable. A slice of nanowood can hold a 1 kg weight without breaking. The material cost for nanowood is about $ 7.44/m^2 and the manufacturing cost is estimated to be low as well due to the simple processing steps such as cutting the wood, soaking the wood in water/chemicals, and freeze drying. The manufacturing process can be compatible with the existing wood-handling and paper industry infrastructure.

discussion S2. Numerical simulations of isotropic and anisotropic thermal insulators

When exposed to a local hot spot, thermal insulation materials with isotropic thermal properties prohibit heat from being effectively dissipated, which causes heat to be locally concentrated near the source. As a result, the temperature contour profile on the front surface shows a circular shape with a maximum temperature of 216 ^{o}C. However, for an anisotropic thermal insulator, heat can be easily transported due to directional high thermal conductivity, which yields an elliptical temperature distribution on the front surface with a maximum temperature of 183 ^{o}C. Similarly, for the intersecting and back-side temperature, the isotropic wood exhibits circular temperature distributions, while the anisotropic wood shows an elliptical shape. From the temperature line profile, the isotropic wood exhibits significant variations in temperature from the edge to the center due to insufficient heat dissipation. The low thermal conductivity in the horizontal direction results in a greater temperature gradient along the line. On the other hand, the anisotropic wood conducts heat more easily in the aligned fibril direction, which results in a more uniform temperature distribution.

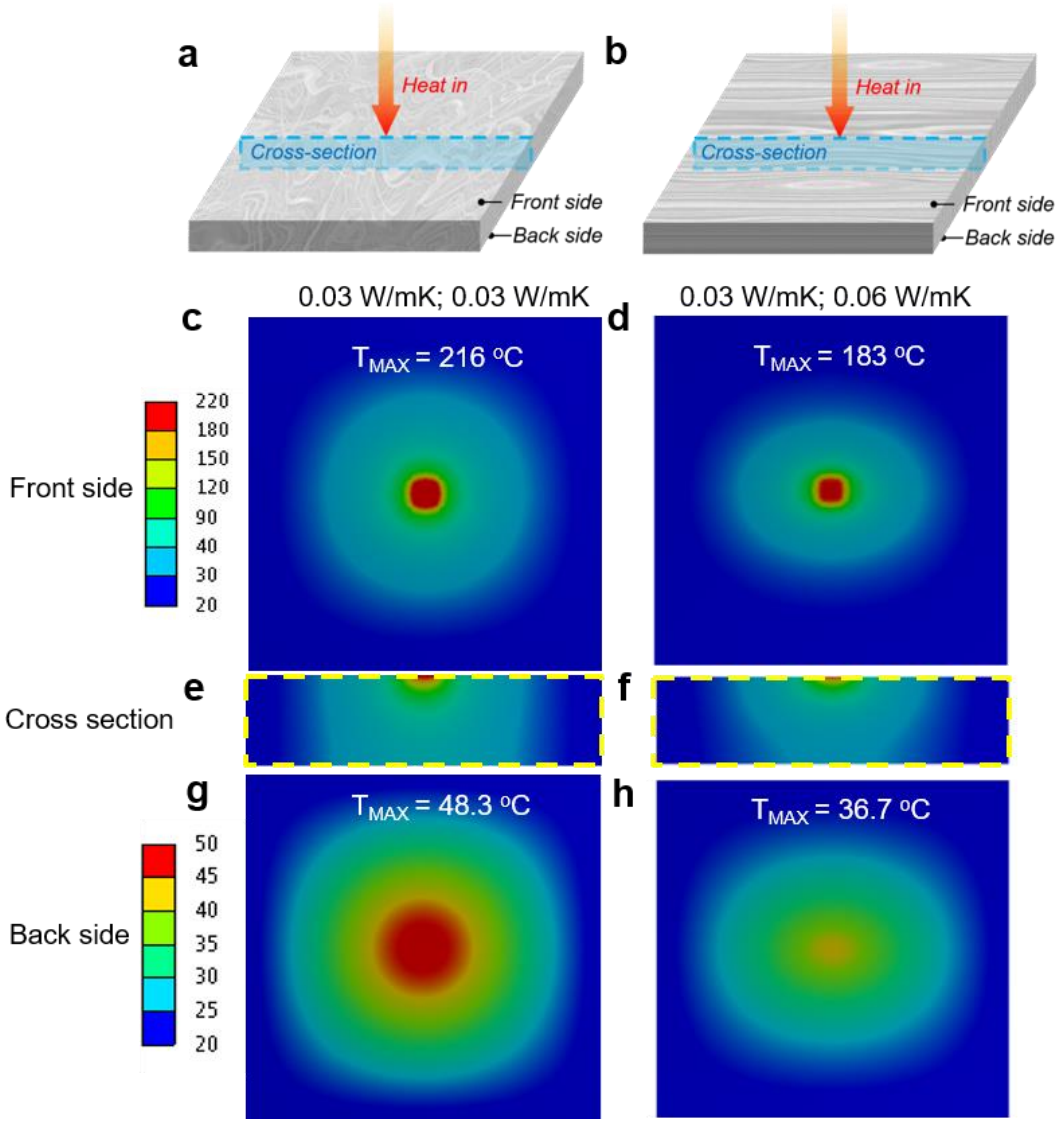

fig. S11. Temperature plots of isotropic and anisotropic thermal insulators from a point heat source. (**a** and **b**) Schematic of the point heat source applied to isotropic and anisotropic thermal insulation materials. The heat source on the top surface dissipates 200 W/m^2 power in the center. A natural convection boundary condition is applied to the peripheral surfaces (ambient temperature of 20 °C, and empirical correlations with temperature dependent convection heat transfer coefficient was applied in the model). (**c** and **d**) Front side surface temperature contour plot of the isotropic and anisotropic thermal insulators. (**e** and **f**) A cross-sectional temperature contour of the isotropic and anisotropic thermal insulators, (**g** and **h**) Back side surface temperature contour plot of the isotropic and anisotropic thermal insulators.

discussion S3. Thermal conductivity estimation

A simple theoretical model(*66*) can be used to estimate the effective thermal conductivity in both the axial and radial directions. Due to the low application temperature, radiative heat transfer is neglected in the following analysis

$$k_{e\perp} = \frac{k_{f\perp} k_g}{(1-\varphi)k_g + \varphi k_{f\perp}} \quad (1)$$

$$k_{e//} = (1-\varphi)k_{f//} + \varphi k_g \quad (2)$$

where φ is the porosity of nanowood, k_g is the thermal conductivity of gas, and $k_{f\perp}$ = 0.766 W/mK and $k_{f//}$ = 0.43 W/mK is the radial and axial thermal conductivity of nanofibril, respectively(*67*, *68*).

The porous nanowood has two levels of porosity (fig. S12): micro-scale channels which range from 10-100 μm in diameter and individual cellulose fibrils which aggregate in the cell walls and exhibit an inter-fibril aggregate spacing in the nanometer range (1-10 nm) (fig. S12).

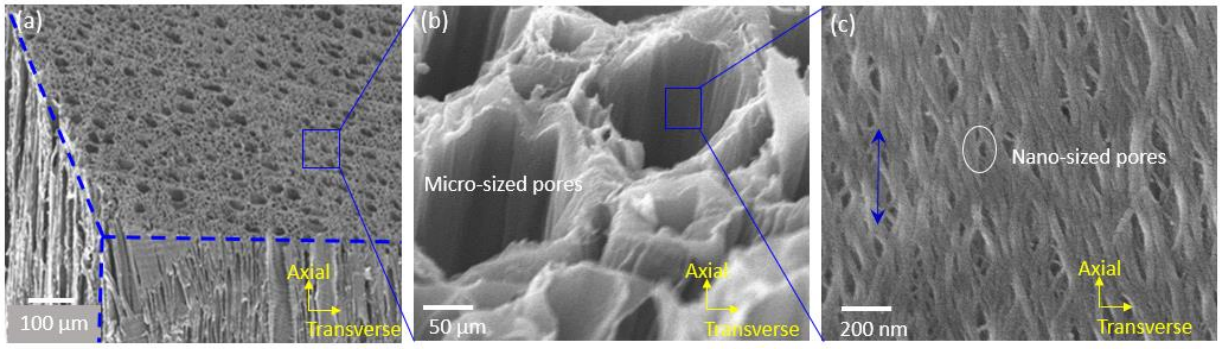

fig. S12. The two levels of porosity (microsized and nanosized pores) in nanowood. (**a**) SEM of the mesoporous structure of nanowood. (**b**) The micro-sized pores (wood lumens) and (**c**) nano-sized pores between nanofibers on the lumen walls. The wood channels and cellulose nanofibers are oriented along wood growth direction.

The thermal conductivity of gas in the confined space nanofibrils can be estimated by(*66*)

$k_g = \frac{k_{g0}}{1 + 2\alpha l/D}$, where k_{g0} = 0.026 W/m·K is the thermal conductivity of gas in the free space, α ≈ 2 for air, l is the mean free path of gas and D is the mean pore size. The mean free path of air is ~70 nm at ambient condition.

<u>In the transverse direction:</u>

Due to abundance of pores with a diameter > 10 µm inside the nanowood, D is much large than l. The effect of the nano-sized pores on reducing the air thermal conduction becomes negligible. Thus, the thermal conductivity of air within 10 to 100 µm sized channels is close to $k_{g0.}$ By taking k_g as $k_{g0,}$ the room temperature thermal conductivity in the radial and axial direction can be calculated to be 0.028 W/m·K, which is close to the experimental value.

<u>In the axial direction:</u>

The parallel model used is a simple model assuming a straight and aligned system with perfectly packed one dimensional channels. However, wood has a complicated mesostructure (fig. S12) and the cellulose fibers are not packed in ideal parallel arrays. There exist pores on the wood cell walls along the axial direction (fig. S12 (c)). Along the axial direction, the gas in the nano-sized pores exhibits a lower thermal conductivity comparable to that of cellulose. Since the model does not consider the pores on the lumen walls in the axial direction, the experimentally obtained thermal conductivity in the axial direction is low compared to the calculated value via the parallel model.

table S1. Materials cost for nanowood production.

Chemicals	Purchase link	Price ($/ton)	Dosage (kg)	Cost ($/m^2)
NaOH	https://www.alibaba.com/product-detail/Fast-shipment-good-quality-Caustic-Soda_60245815362.html?spm=a2700.7724838.0.0.pfCdx9	300	5.2	1.56
Na_2SO_3	https://www.alibaba.com/product-detail/High-quanlity-white-powder-Anhydrous-Sodium_60464778943.html?spm=a2700.7724838.0.0.uw2CnM	300	2.6	0.78
H_2O_2	https://www.alibaba.com/product-detail/HYDROGEN-PEROXIDE_60350827959.html?spm=a2700.7724838.0.0.mubFtS&s=p	300	12.5	3.75
Basswood	https://detail.1688.com/offer/527306702834.html	135 $/m^3	0.01 m^3	1.35
Total (Nanowood)				**7.44 ($/m^2)**

discussion S4. Thermal stability of nanowood

Our literature study shows that cellulose pyrolysis occurs within a temperature range of 315 ^{o}C to 400 ^{o}C, while hemicellulose decomposes easily between 220 ^{o}C and 315 ^{o}C, and lignin decomposition occurs from ambient temperatures to 900 ^{o}C. For cellulose, the maximum weight loss range (2.84 wt. %/^{o}C) was attained at 355 ^{o}C while the value is < 0.1 wt. %/^{o}C from ambient temperature to 300 ^{o}C (*69*).

We performed thermogravimetric analysis of both the original and delignified wood. Compared with original wood (43.8% cellulose, 20.1% hemicellulose, 21.1% lignin, from compositional analysis), the delignified wood (37.8 % cellulose, 2.3 % hemicellulose, 0.1 % lignin, from compositional analysis) is mainly composed of cellulose. As can be observed, delignified wood exhibits much slower mass loss around 315 ^{o}C compared with original wood and the mass is more stable at elevated temperatures. It is well known that cellulose is more stable < 100 ^{o}C compared with original wood (*69*). Consequently, the delignified wood can be widely applied to areas where wood is used (e.g. building materials).

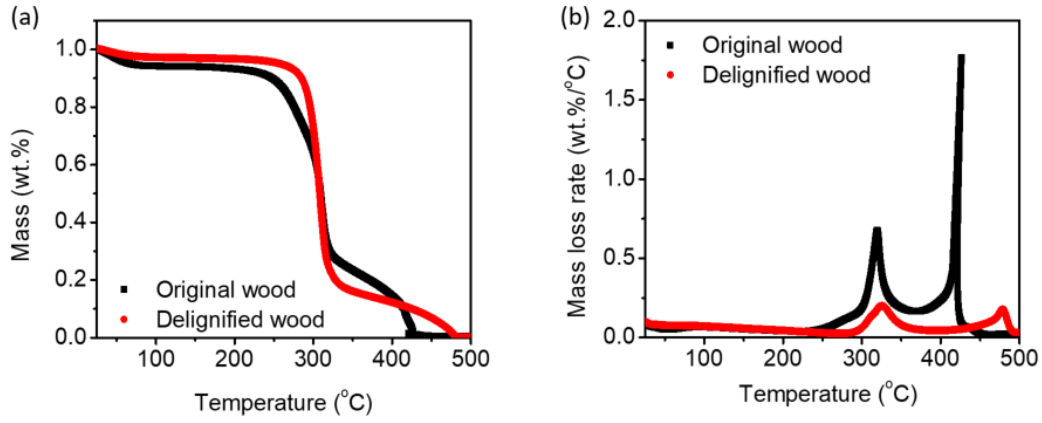

fig. S13. Thermogravimetric analysis. (**a**) Mass and (**b**) rate of mass loss of the original and delignified wood.

The fabricated delignified wood shows no appreciable color or morphology change after ~14 months in the ambient environment (fig. S14).

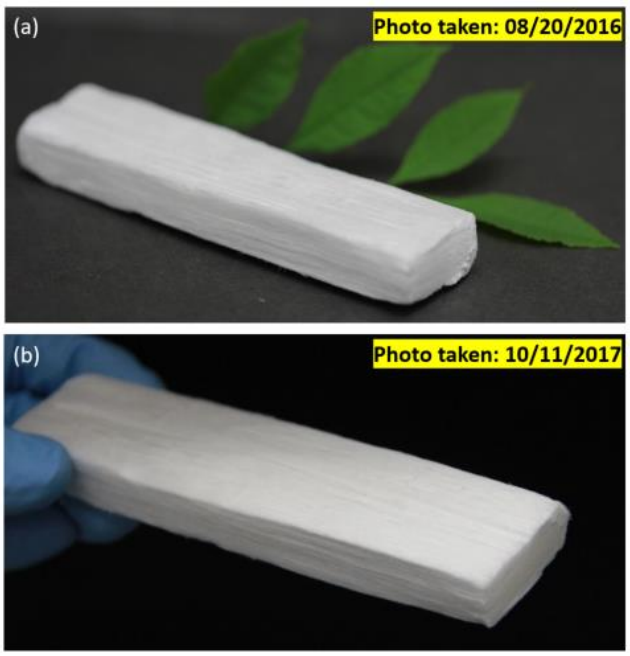

fig. S14. Digital images of the delignified wood piece after >1 year under ambient environment. Images of the delignified wood taken (**a**) after fabrication (08/20/2016) and (**b**) recently (10/11/2017), confirming the morphological stability after 14 months under ambient conditions.

discussion S5. Permeability of nanowood

We used a home-made set-up to test the air permeability of the nanowood in the traverse direction (the direction of air passage when applied as scalable building material). One side of the glass tube was sealed with the nanowood and pressure was added on the other side of the glass tube. The air permeability results of the nanowood are shown in fig. S15. The nanowood is breathable which is critical to achieve improved indoor air quality.

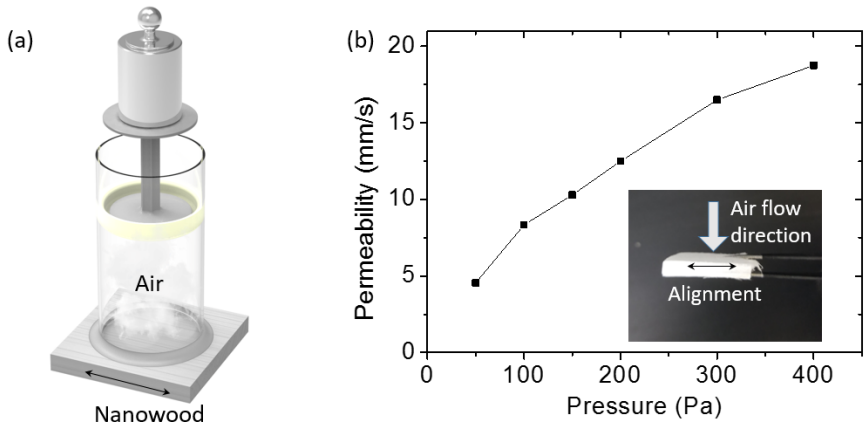

fig. S15. Air permeability test of nanowood. (**a**) Setup of the air permeability test. (**b**) Air permeability results in the transverse direction of the nanowood.

discussion S6. Scalable manufacturing

The wood board used in the fabrication of nanowood is cut along the wood growth direction, which is compatible with large-scale wood cutting processes. The common cutting procedure adapt by industry is to peel the wood block with a desirable thickness and then pressed the boards flat (fig. S16). The scalability, cost-effectiveness, and performance renders our nanowood attractive for various applications.

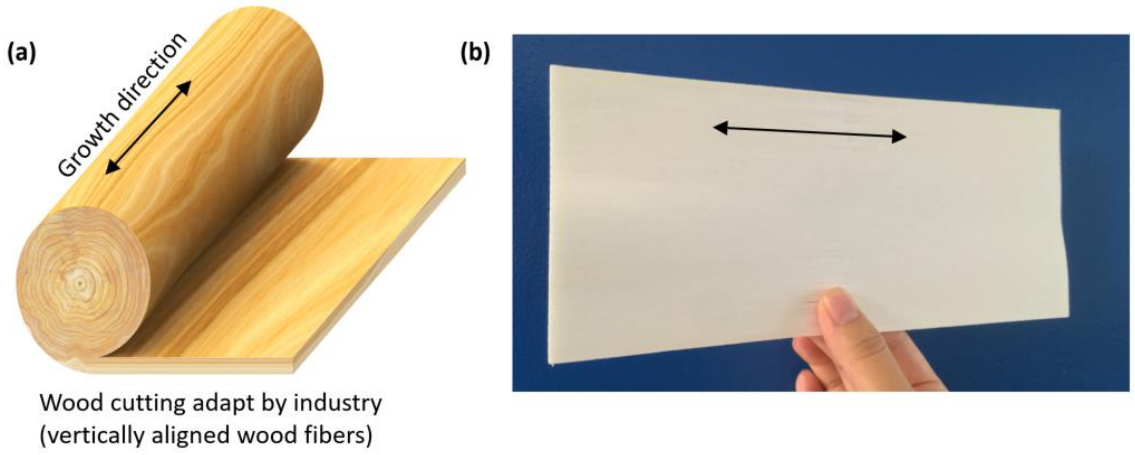

fig. S16. Industry compatible wood board cutting method. (**a**) The wood cutting method to produce vertically aligned wood panels is compatible with the industry-adapted Swiss roll cutting method. (**b**) Image of a wood panel after the delignification process.

discussion S7. Comparison with a stack of paper and honeycomb wrapping paper

Honeycomb paper wraps are made by cutting and pasting paper strips together. The pores are typically of the centimeter range, which is not comparable with nanowood. The material properties of the honeycomb paper wrap depend on the paper used for cutting and pasting. The mechanical strength of a stack of paper for bulk application will also depend on the adhesives between each sheet.

1. Mass density: The nanowood exhibits a lower mass density (0.13 g/cm^3) compared with most of types of papers due to the large porosity of the hierarchal structure. Paper is composed of cellulose fibers that are pressed flat (1.20 g/cm^3).

2. The alignment of cellulose nanofibers in nanowood results in a large interaction area between chains, which increases the bonding between cellulose fibers and leads to high mechanical strength. In comparison, in typical paper making, the delignification process requires mechanical and chemical disintegration of the cellulose fibers, resulting in randomly distributed and degraded cellulose fibers, resulting in a much lower mechanical strength.

3. The cellulose fibers in paper have been pressed flat. The mesostructure of paper cannot sustain a porous backbone. Thus, the thermal conductivity is reported to be much higher than nanowood (*70*).

4. The delignification process totally destroys the anisotropic nature of cellulose in pristine wood in paper making, which results in a randomized fiber orientation. Our method of fabrication aligned cellulose fibers is facile yet effective. This is the first report on making massive arrays of aligned cellulose fibers for high volume and low-cost

applications.

5. The anisotropic properties result from the structural merit of the aligned cellulose fibers. Paper doesn't exhibit anisotropy owing to the randomized fiber alignment resulting from the bottom-up process.

Nanowood is a 3-dimensional material which can be used for bulk applications such as energy efficient building materials. For building applications, paper from delignified wood has the following challenges: (1) it is thin, and not a bulk material for construction applications; (2) stacking requires additional adhesive; (3) poor mechanical strength; (4) processing wood into paper is time consuming and energy intensive, not suitable for building applications that require large volume with extremely low cost per mass.

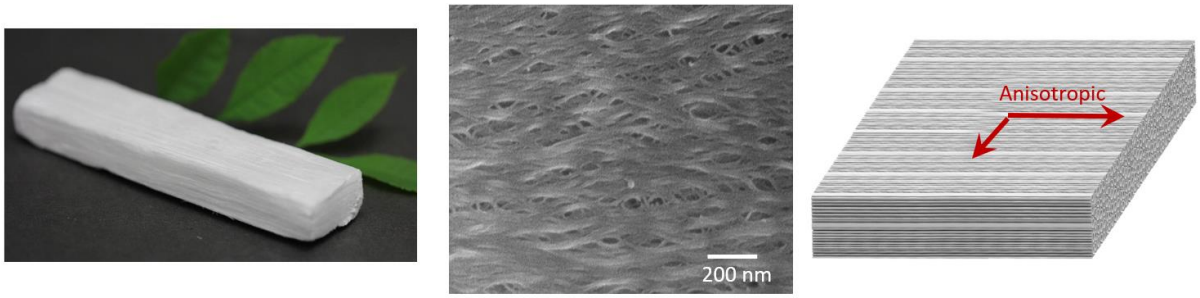

fig. S17. Nanowood is composed of aligned cellulose nanofibers with mesoporous structure.

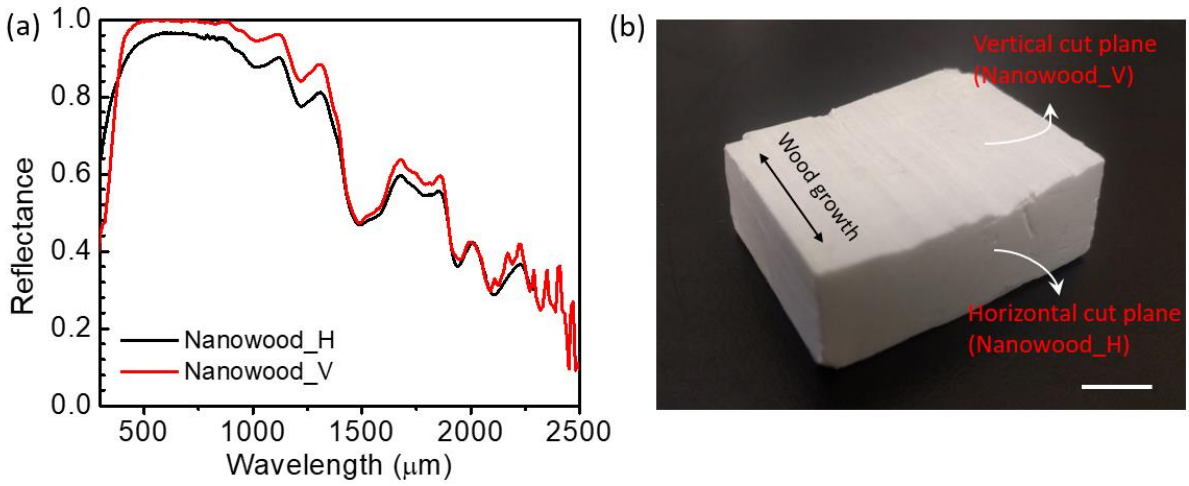

fig. S18. Reflectance comparison between vertically cut plane and horizontally cut plane of nanowood. (**a**) Reflectance comparison between vertically cut plane (Nanowood_V) and horizontally cut plane (Nanowood_H). (**b**) Image of the sample used for the reflectance measurement. Scale bar: 1 cm. Reflectance of the Nanowood_H is slightly lower than that of the Nanowood_V due to the increased light trapping of the porous structure with the horizontal cut. Scale bar: 1 cm. Note heat mainly radiates on the Nanowood_V in practical thermal insulation applications.

table S2. Comparison between nanowood, paper, and honeycomb paper wraps.

	Nanowood	**Paper**	**Honeycomb paper wraps** (made from paper sheet by cutting and pasting)
Mass density	0.13 g/cm^3	1.20 g/cm^3	NA (depends on the cutting and pasting process)
Mechanical strength (Tensile)	18 MPa	250 – 300 KPa (*65*)	NA (depends on the adhesives)
Thermal conductivity	0.03 W/m·K	0.07 ~ 0.18 W/m·K (*70*)	0.07 ~ 0.18 W/m·K (*70*)
Fiber orientation	Aligned	Random	Random
Anisotropic	Yes	No	No
Capability for bulk applications	Yes	No	No

discussion S8. The effect of humidity

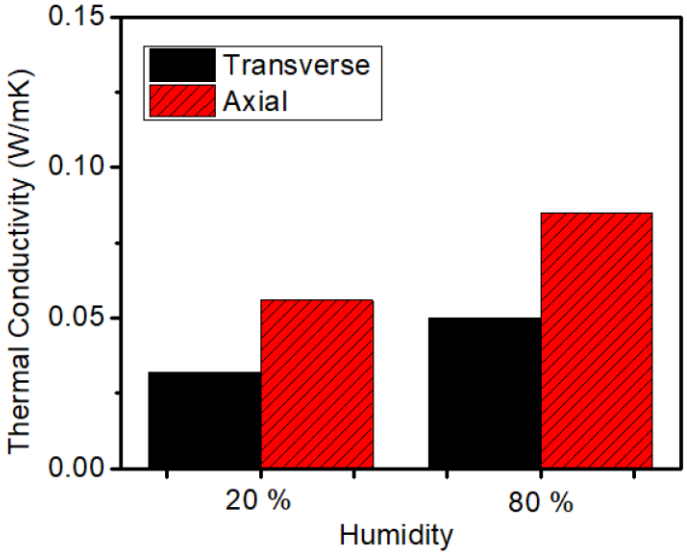

fig. S19. Thermal conductivity in transverse and axial direction under humidity of 20% and 80%, respectively.

The mechanical properties under 80% humidity is compared to that under 20% humidity. The sample was stored at the respective humidity for at least 24 hours before the measurement. As expected, the mechanical strength decreases with the increase in humidity.

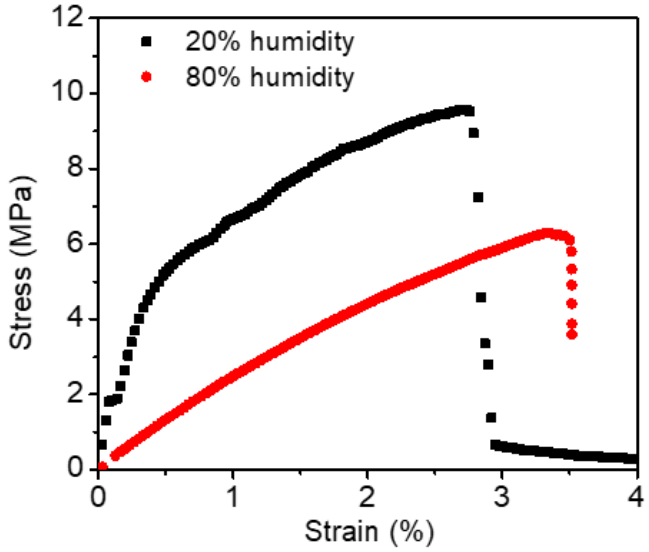

fig. S20. The tensile strength of nanowood under 20 and 80% humidity.